Published in final edited form as:
Mech Dev. 2007 ; 124(9-10): 746–761.

A dosage-dependent role for *Spry2* in growth and patterning during palate development

Ian C. Welsh, **Aaron Hagge-Greenberg**, and **Timothy P. O'Brien***
Department of Biomedical Sciences, Cornell University, Ithaca NY

Abstract

The formation of the palate involves the coordinated outgrowth, elevation and midline fusion of bilateral shelves leading to the separation of the oral and nasal cavities. Reciprocal signaling between adjacent fields of epithelial and mesenchymal cells directs palatal shelf growth and morphogenesis. Loss of function mutations in genes encoding FGF ligands and receptors have demonstrated a critical role for FGF signaling in mediating these epithelial-mesenchymal interactions. The Sprouty family of genes encode modulators of FGF signaling. We have established that mice carrying a deletion that removes the FGF signaling antagonist *Spry2* have cleft palate. We show that excessive cell proliferation in the *Spry2*-deficient palate is accompanied by the abnormal progression of shape changes and movements required for medially-directed shelf outgrowth and midline contact. Expression of the FGF responsive transcription factors *Etv5*, *Msx1*, and *Barx1*, as well as the morphogen *Shh*, is restricted to specific regions of the developing palate. We detected elevated and ectopic expression of these transcription factors and disorganized *Shh* expression in the *Spry2*-deficient palate. Mice carrying a targeted disruption of *Spry2* fail to complement the craniofacial phenotype characterized in *Spry2* deletion mice. Furthermore, a *Spry2*-BAC transgene rescues the palate defect. However, the BAC transgenic mouse lines express reduced levels of *Spry2*. The resulting hypomorphic phenotype demonstrates that palate development is *Spry2* dosage sensitive. Our results demonstrate the importance of proper FGF signaling thresholds in regulation of epithelial-mesenchymal interactions and cellular responses necessary for coordinated morphogenesis of the face and palate.

1. Introduction

Facial morphogenesis requires the coordinated outgrowth, patterning and fusion of multiple structures. Paired facial primordia, derived from the first branchial arch, give rise to the mandibular and maxillary arches that extend and join at the midline with the frontonasal process to frame the lower jaw, upper jaw and face. A more recent evolutionary advance is the secondary palate, formed by the outgrowth and midline fusion of bilateral maxillary shelves to separate the oral and nasal cavities. The palatal shelves are an elongated bud-like outgrowth of maxillary mesenchyme covered by an epithelial sheet. During mouse development proliferative expansion of the cranial neural crest derived mesenchyme results in the initial vertical extension of the palatal shelves to a position lateral to the tongue. Following this initial phase of vertical growth, midline contact of the bilateral shelves is achieved by a combination

*Corresponding author: Timothy P. O'Brien Department of Biomedical Sciences Cornell University Ithaca, New York 14853 (607) 253-4326 (phone) (607) 253-4495 (fax) tpo5@cornell.edu (email)

of rotation and elevation movements as well as medially directed growth. Contact between the bilateral shelves is typically initiated in the mid palate region first where the vertical shelves swing dorsally into close apposition above the tongue. In the anterior and more posterior palatal shelf, contact requires more extensive tissue reshaping to orient outgrowth towards the midline (Chou et al., 2004; Sakamoto et al., 1989). Upon midline contact from E14.5-E15.5 remodeling and fusion removes the medial epithelial seam in order to form a continuous palate (Ferguson, 1988). Concurrent with these morphogenic processes, fields of cells must also be directed to exit the cell cycle in order to initiate skeletogenic differentiation to form the bony processes of the hard palate that extend from the maxilla and palatine bones. These bones arise from mesenchymal condensations from which cells directly differentiate into bone forming osteoblasts, a process known as intramembranous ossification. Mutations that alter regulation at any stage of this complex developmental process can lead to prominent birth defects including clefting of the lip and secondary palate.

The outgrowth of bud-like structures such as the palatal shelves is regulated via interactions between the overlying epithelium and underlying mesenchyme. These epithelial-mesenchymal interactions are mediated by growth-factor dependent signaling pathways in order to provide instructive cues necessary to coordinate a range of cellular behaviors. For example, the fibroblast growth factor (FGF) and bone morphogenetic protein (BMP) signaling pathways control cellular responses including changes in gene expression, cell adhesion, proliferation, and survival. Furthermore, regional domains in the facial primordia and palate are defined by differences in gene expression in response to these signaling pathways with consequences for the growth and patterning along the anterior-posterior axis of the palate (Hilliard et al., 2005). *Msx1* and *Barx1* are two homeobox transcription factors involved in the morphogenesis of several craniofacial elements (Barlow et al., 1999; Bei and Maas, 1998; Satokata and Maas, 1994; Tucker et al., 1998a). Distal *Msx1* and proximal *Barx1* expression in the mesenchyme of the first branchial arch is maintained in the developing maxilla to form complementary anterior *Msx1* and posterior *Barx1* expression domains in the palatal shelves (Barlow et al., 1999). *Msx1* expression in the anterior palate has been shown to depend on *Bmp4* (Zhang et al., 2002). However, *Msx1* is known to be a downstream target of both BMP and FGF signaling in various developmental contexts. It has also been demonstrated that *Barx1* expression is regulated by FGF and BMP signaling. For example, local inhibition of BMP4 signaling results in FGF associated ectopic expression of *Barx1* in the distal mandible and leads to transformation of the distal incisor to a proximal molar tooth phenotype (Tucker et al., 1998b). Thus, rather than pathway specific input, the patterning of the proximal-distal axis of the branchial arch and subsequent anterior-posterior axis of the palatal shelf into domains of *Msx1* and *Barx1* expression is likely dependent on the relative local strength of BMP and FGF signaling.

Negative feedback or inhibitory interactions play a critical role in setting the relative strength of various signaling pathways. Elucidating the role of specific inhibitors in defining signaling domains and thresholds will provide insights into the cellular signaling mechanisms that direct orofacial development. FGF signaling is antagonized by *sprouty* (*spry*), an intracellular inhibitor of the receptor tyrosine kinase (RTK) pathway, identified as a negative regulator of airway branching in *Drosophila* (Hacohen et al., 1998). SPRY antagonistic activity is evolutionarily conserved and the expression of *Spry1*, *Spry2* and *Spry4* overlaps with FGF signaling domains during mouse development including developing craniofacial structures (Minowada et al., 1999). The FGF signaling pathway plays a central role in reciprocal interactions between adjacent tissues during diverse morphogenic processes including palate and facial development (Thisse and Thisse, 2005). Several members of the FGF family of ligands and their receptors including *Fgf8*, *Fgf9*, *Fgf10*, *Fgf18*, *Fgfr1*, and *Fgfr2* are specifically expressed in either the oral epithelium or mesenchyme during craniofacial morphogenesis and when mutated lead to cleft palate (Alappat et al., 2005; Colvin et al., 2001; Liu et al., 2002;

Rice et al., 2004; Trokovic et al., 2003; Trumpp et al., 1999). The craniofacial defects that result from mutations in these genes are often associated with haploinsufficient or variably penetrant phenotypes. This further highlights the importance of establishing the proper FGF signaling dose in the regulation of these processes.

Phenotypic analysis of targeted mutations has demonstrated a requirement for vertebrate *Sprouty* genes during kidney morphogenesis, differentiation of the auditory epithelium, regulation of odontogenesis, limb patterning, and enteric neuron development (Basson et al., 2005; Hansen et al., 2003; Klein et al., 2006; Shim et al., 2005; Taketomi et al., 2005). In addition, disruption of both *Spry2* and *Spry4* results in severe defects in craniofacial, limb, and lung morphogenesis (Taniguchi et al., 2007). In this study we examine the connection between *Spry2* function and FGF signaling interactions that are involved in palate and facial development. We show that palate morphogenesis is disrupted in mice homozygous for a Mb-scale deletion that removes the *Spry2* locus. Abnormal palate development is marked by excessive cell proliferation and the misexpression of FGF-responsive genes. We also establish that a targeted disruption of *Spry2* fails to complement the cleft palate phenotype uncovered by the *Spry2*-deletion allele. In addition, *Spry2*-BAC transgenic mouse lines expressing reduced levels of *Spry2* show complete rescue of facial clefting and dosage-dependent rescue of the palatal defect. The sensitivity of palate development to *Spry2* dose highlights the importance of proper regulation of FGF signaling thresholds necessary to coordinate the timing of craniofacial development.

2. Results

2.1. Spry2 deficient mice exhibit palate and facial clefting

We identified *Spry2* as a candidate gene for craniofacial defects in mice homozygous for the *Ednrb*$^{s\text{-}36Pub}$ (hereafter, *36Pub*) deficiency of the piebald deletion complex (Peterson et al., 2002; Roix et al., 2001). The piebald deletion complex is a collection of overlapping Mb-scale chromosomal deficiencies centered around the endothelin receptor B (*Ednrb*) coat color spotting locus on distal mouse chromosome 14 (Mmu14). We have used the piebald deletions to uncover several loci essential for mammalian development. *36Pub* deletion homozygotes (*36Pub*−/−) have a high incidence (83%) of cleft secondary palate and a lower incidence (27%) of cleft lip (Table 1). The genetically defined ~1 Mb *36Pub* critical interval completely removes the FGF signaling antagonist *Spry2* as well as two other genes, *Rbm26* and *Ndfip2*, ~600 Kb proximal to *Spry2* (Peterson et al., 2002). Based upon the nature of the *36Pub* palate phenotype and the established role of FGF signaling in the regulation of cellular proliferation of both the epithelium and mesenchyme during palate development we prioritized *Spry2* as a candidate gene within the *36Pub* critical interval (Rice et al., 2004).

We have further characterized the developmental basis of the clefting defects associated with the *36Pub* mutant mouse. We compared serial frontal sections from E13.5 to E15.5 embryos to identify differences in the developmental progression of the wildtype and mutant palatal shelves. Palatal shelf morphology between mutant and wildtype embryos was comparable at E13.5 (data not shown). However, by E14.5 clear differences in the morphology of the *36Pub* mutant were apparent, particularly in the mid to posterior palate. The shelves of the E14.5 wildtype palate had elevated dorsal to the tongue and contacted in the mid palate (Fig. 1A-D). In contrast, the mutant shelves remained positioned lateral to the tongue in the anterior and middle region (Fig. 1E-F). Additionally, shape changes associated with the directed growth of the wildtype palate were altered in the mutant. Specifically, the distinct medially projecting prominence seen along the posterior palate and soft palate (Fig. 1C-D) was absent in the mutant (Fig. 1G-H). Instead, it appeared that the posterior region of the E14.5 mutant palate had failed to transition from the vertically directed growth that is more typical of E13.5 embryos. By E15.5 the palatal shelves of the wildtype embryo were in contact along their entire length and had nearly completed fusion as evidenced by the loss of the medial edge epithelium (Fig. 1I-L). Although the posterior half of the E15.5 mutant palate did show limited evidence of redirected growth towards the midline the anterior shelves had not elevated, possibly due to obstruction by the tongue (Fig. 1M-P). We observed that the morphology of the posterior palate of mutants is markedly altered even when compared to E14.5 wildtype embryos whose palates have not yet elevated (see Fig. 5). These observations suggest that medially directed growth of the posterior palate over the tongue may play a more significant role in the mechanical elevation of the palate than has been previously appreciated.

2.2. Dynamic expression of Spry2 and components of the FGF signaling pathway in the facial primordia and palate

To further evaluate the role of *Spry2* during craniofacial development we examined its expression pattern during early facial morphogenesis. In embryos from E9.5 to E11.5 *Spry2* was expressed in known FGF signaling domains of the developing facial primordia including the frontonasal process and maxillary and mandibular components of the first branchial arch (Fig. 2A&B). *Spry2* was also dynamically expressed in the epithelium and mesenchyme throughout palate development. At E12.5 *Spry2* is expressed in the anterior palate in the mesenchyme and overlying epithelium. In the E14.5 pre-fusion palate *Spry2* expression becomes more restricted to the epithelium on the oral surface of the mid-palate, and along the medial aspect of the approaching palatal shelves with notably intense expression in the posterior half of the palate (Fig. 2C-D).

We next compared *Spry2* expression during palate development in relation to the expression of other components of the FGF signaling pathway (Fig. 2E-T). FGF10 signaling has been shown to be critical for coordinating epithelial-mesenchymal interactions during the morphogenesis of several embryonic structures including the palate, limb, and lung (Min et al., 1998; Revest et al., 2001; Rice et al., 2004). Cleft palate due to the loss of *Fgf10* function is associated with reduced proliferation throughout the palatal epithelium and to a lesser extent in the mesenchyme as well as increased apoptosis in the medial edge epithelium (MEE) (Rice et al., 2004). From E11.5 to E14.5 *Fgf10* is expressed in the mesenchyme of the anterior two-thirds of the palate in a domain that will become the future hard palate. As development progresses from E12.5 to E13.5 *Fgf10* expression becomes ventrally restricted to the oral side of the palate while maintaining a posterior boundary at the level of the molar tooth buds (Fig. 2E, I, J, & K).

Bidirectional FGF signaling between the epithelium and mesenchyme of the palate is mediated by fibroblast growth factor receptor 2 (*Fgfr2*). Alternative splicing of FGFR2 results in expression of epithelial specific FGFR2IIIb and mesenchymal specific FGFR2IIIc isoforms. Cleft palate due to specific loss of function of the *Fgfr2b* isoform demonstrates its role as the major receptor for mesenchymal FGF10 signaling (De Moerlooze et al., 2000; Rice et al., 2004). *Fgfr2c* isoform expression is required in early mesenchymal condensations to regulate normal osteoprogenitor cell proliferation and differentiation (Eswarakumar et al., 2002). An engineered gain of function mutation in *Fgfr2c* impacts osteoprogenitor differentiation and also results in cleft palate (Eswarakumar et al., 2004). We performed *in situ* hybridization using an antisense probe that recognizes both the IIIb and IIIc isoforms of *Fgfr2* (Fig. 2F, L, M, & N). At E13.5, *Fgfr2b* is strongly expressed in the epithelium along the anterior-posterior length of the palate on both the oral and nasal side. Consistent with its role in osteoblast specification and differentiation, *Fgfr2c* signal at E13.5 was found in osteogenic regions prior to overt mesenchymal condensation in the anterior maxilla and along the medial aspect of the vertical palatal shelf adjacent to the nasal epithelium.

The ETS family of signal dependent transcription factors are known to mediate FGF/RTK signaling and their activity is regulated by phosphorylation by MAPK (Sharrocks, 2001).

Etv5 is a member of the *Pea3* subfamily of ETS transcription factors and as a direct transcriptional target of FGF/RTK signaling the expression pattern of *Etv5* provides a report of the spatial activity of this signaling pathway. In the E13.5 palate, *Etv5* is expressed in a broad domain within the anterior mesenchyme that becomes medially restricted in the mid-posterior palate to a domain encompassing that of *Fgfr2c* (Fig. 2H, R, S, & T). In the palatal epithelium, *Etv5* is robustly expressed on the oral surface of the palatal shelf with a sharp medial boundary. *Etv5* expression is not found in the MEE or in the nasal surface epithelium of the palatal shelf (Fig. 2R&S).

Spry2 expression largely overlaps that of *Etv5* in the E13.5 palate with some key differences (Fig. 2G, O, P, & Q). In the anterior and posterior mesenchyme, *Spry2* is more broadly expressed along the mediolateral axis of the palatal shelf, whereas in the mid palate expression is more tightly restricted to the medial aspect of the shelf within the domain of *Fgfr2c* expression. Furthermore, although the most robust expression of *Spry2* in the epithelium overlaps with *Etv5* on the oral surface it is expressed throughout the MEE and nasal side epithelium as well, implying differential regulation of FGF signaling strength along the medial aspect of the vertical shelf. The complementary and overlapping expression domains of *Spry2* with other components of the FGF pathway in the palate highlight the reciprocal nature of FGF signaling during palate development and show a strong correlation with the phenotype of the *Spry2*-deficient *36Pub* mutants.

2.3. Complementation testing and a Spry2-BAC transgenic rescue with a hypomorphic phenotype

A role for *Spry2* in palate and facial development is indicated by its expression pattern, activity as an FGF inhibitor, and the craniofacial defects observed in the *Spry2* deficient, *36Pub* deletion mutant mice. A targeted mutation of *Spry2* (*Spry2*$^{\Delta\mathrm{ORF}}$) has recently been reported that demonstrates a critical role for *Spry2* in postnatal viability, differentiation of the auditory epithelium, and restricting responsiveness to epithelial-mesenchymal FGF signaling during early tooth development (Klein et al., 2006; Shim et al., 2005). However, palate defects have not been reported in *Spry2*$^{\Delta\mathrm{ORF}}$ loss of function mice. In order to determine whether *Spry2* contributes to the craniofacial defects associated with the 36*Pub* deletion we performed a complementation cross using 36*Pub* deletion and *Spry2*$^{\Delta\mathrm{ORF}}$ mice. We scored palate closure at E18.5 in the progeny of intercrosses of *Spry2*$^{\Delta\mathrm{ORF}}$ and *36Pub* heterozygous animals. We observed clefts of the secondary palate in 6 of 17 (35%) 36*Pub/ Spry2*$^{\Delta\mathrm{ORF}}$ compound mutants (table 1), indicating a failure of the *Spry2*$^{\Delta\mathrm{ORF}}$ mutation to complement craniofacial defects associated with the 36*Pub* deletion.

We also used a BAC transgenic approach to further evaluate *Spry2* function during palate development. We tested whether a *Spry2*-BAC transgene could complement the craniofacial defects associated with the *36Pub* deletion. Computational gene prediction (e.g. GRAIL), similarity searches against gene, EST and protein databases and comparative analysis of mouse and human genomic sequences support that the centrally located *Spry2* is the only gene contained on the 80 Kb BAC used in these experiments (Peterson et al., 2002). Seven *Spry2*-BAC transgenic founders were generated. Analysis using markers that are polymorphic between the 129-derived BAC sequences and the C57BL/6J host genome revealed that portions of the *Spry2*-BAC had been deleted in two of the transgenic lines. The remaining five lines were used to generate offspring that were hemizygous for the *Spry2*-BAC transgene and homozygous for the *36Pub* deletion (*36Pub*−/−, *Spry2*-Tg). This permitted the *Spry2* expression pattern and levels derived from the *Spry2*-BAC transgene to be analyzed in the absence of endogenous *Spry2* expression.

The expression of *Spry2* in each of the BAC transgenic lines was initially examined by *in situ* hybridization in E10.5 36*Pub*−/−, *Spry2*-Tg embryos. Two transgenic lines (2 and 69) were selected that expressed readily detectable levels of *Spry2* in a pattern comparable with endogenous *Spry2*. E10.5 36*Pub*−/−, *Spry2*-Tg-2 and 36*Pub*−/−, *Spry2*-Tg-69 embryos showed expression of *Spry2* in regions including the developing CNS, limb buds and facial primordia (Fig. 3A-C). We also examined embryos at later stages to document expression in the developing palate. *Spry2* expression was detected in the palatal tissue of E13.5 to E15.5 36*Pub*−/−, *Spry2*-Tg embryos in a pattern comparable to that seen in normal embryos (Fig. 3D-F). Although the expression pattern from the *Spry2*-BAC-2 and 69 transgenes was similar to that of the endogenous locus, the level of expression was diminished. We performed quantitative RT-PCR analysis to examine the expression level of *Spry2* in the BAC transgenic lines compared with the endogenous locus. Quantitative expression studies focused on the E14.5 palate and showed that BAC transgenic line 2 expressed *Spry2* at ~12.5% and line 69 at ~25% of wildtype levels (Fig. 3G).

Although the *Spry2*-BAC transgenic lines express reduced levels of *Spry2*, we tested the ability of each transgene to rescue defective facial and palate development in 36*Pub* deletion mutant mice. Both *Spry2*-BAC transgenic lines 2 and 69 completely rescued the 27% incidence of cleft lip in the 36*Pub* mutant mice (Fig. 4A,B, & C, and Table 1). Mice representing both of the *Spry2*-BAC transgenic lines examined at E18.5 showed that rescue of the cleft palate phenotype is dosage-sensitive. The incidence of cleft palate was reduced to 42% in 36*Pub*−/−, *Spry2*-BAC-2 transgenic mice, while in the 36*Pub*−/−, *Spry2*-BAC-69 transgenic mice the incidence of cleft palate was further reduced to 8% (Fig.4D, E, & F, and Table 1). Thus, the reduced levels of expression in the *Spry2*-BAC transgenic mice are associated with the hypomorphic phenotype of incompletely penetrant palate clefting.

2.4. Misexpression of FGF-responsive genes and altered palatal shelf patterning in the absence of Spry2

FGF signaling defines gene expression domains during facial development (Bachler and Neubuser, 2001; Francis-West et al., 1998; Shigetani et al., 2000; Trumpp et al., 1999). We examined FGF-responsive genes for misexpression resulting from the loss of *Spry2*. The ETS transcription factor family member *Etv5* is regulated by FGF signaling during development of the face (Firnberg and Neubuser, 2002). Compared to control littermates, *36Pub* mutants show a persistent upregulation and expansion of *Etv5* throughout the anterior oral epithelium from E13.5 to E14.5 (Fig. 5A-D). At E13.5 *Etv5* is also expressed in the mesenchyme along the A-P axis in the medial aspect of the vertical shelf with only the posterior most region of the future soft palate lacking *Etv5* expression. By E14.5 the posterior limit of this domain is shifted anteriorly such that only the anterior two thirds of the palate show mesenchymal *Etv5* expression (Fig. 5A&C). In E13.5 *36Pub* mutants this mesenchymal *Etv5* expression appears elevated and by E14.5 extends ectopically into the posterior limit of the palatal shelf (compare Fig. 5A&C with 5B&D). These results are consistent with elevated and expanded FGF signaling activity due to the loss of *Spry2* antagonism in the *36Pub* mutant palate.

The homeobox transcription factor *Barx1* is induced by FGF8 in the proximal mesenchyme of the E10.5 first branchial arch (Trumpp et al., 1999). The extent of the *Barx1* expression domain in the maxillomandibular region and the resulting patterning of the facial primordia is determined by the balance of FGF/BMP signaling (Barlow et al., 1999; Shigetani et al., 2000). We therefore examined the impact of altered FGF signaling thresholds due to the loss of *Spry2* on *Barx1* expression. In E13.5 *36Pub* mutants *Barx1* expression in the anterior epithelium is upregulated and expanded. The *Barx1* expression domain in the posterior mesenchyme of E13.5 *36Pub* mutants is also expanded, both anteriorly and medio-laterally, into domains that normally show lower levels of *Barx1* expression in wildtype embryos. Of particular note is the elevated expression in the medial aspect of the posterior palate where the subsequent altered morphology of the E14.5 mutant palate is most evident (arrows in Fig. 5E

& F and dashed lines in E14.5 palates in Fig. 5). Persistent upregulated *Barx1* expression is still evident at E14.5 to E15.5 (Fig. 5H and data not shown).

Msx1 in the anterior palate is a critical part of a BMP4-responsive pathway central to mesenchymal cell proliferation (Zhang et al., 2002). In certain contexts, *Msx1* expression is also regulated by FGFs, for example in the developing tooth and cranial sutures (Alappat et al., 2003; Bei and Maas, 1998; Kettunen and Thesleff, 1998; Kim et al., 1998). Although bead implantation studies have demonstrated that FGF is able to induce *Msx1* expression in palatal mesenchyme, *Msx1* expression is unaltered in *Fgf10*−/− mutant palates (Alappat et al., 2005; Rice et al., 2005). Therefore, it remains unclear whether *Msx1* expression in the palatal mesenchyme is also jointly regulated by BMP and FGF signaling. In the anterior palate the FGF antagonist *Spry2* may act to restrict the role that FGF signaling plays in *Msx1* expression. In support of this hypothesis, we found that *Msx1* expression in the anterior palate is elevated in *Spry2*-deficient *36Pub* mutants at E13.5 (Fig. 5 I&J). Persistent elevated *Msx1* expression is still evident in E14.5 mutant palates when compared to wildtype (Fig. 5 K&L). Furthermore, the posterior boundary of the normally anteriorly restricted *Msx1* is seen to ectopically extend into the mid-posterior palate of *36Pub* mutants (Fig. 5 I-L).

Mutations in the T-box containing transcription factor *Tbx22* are frequently associated with X linked cleft palate and ankyloglossia, an abnormal thickening of the frenulum of the tongue that restricts its mobility (Marcano et al., 2004). During palate development, *Tbx22* shows restricted expression to the middle and posterior mesenchyme (Fig. 5M), a region significantly altered in *Spry2*-deficient palates. As the posterior palate of the E14.5 wildtype initiates medially directed outgrowth, the domain of *Tbx22* also expands to become expressed throughout the medial aspect of the posterior third of the palate (Fig. 5O). Expression of *Tbx22* in E13.5 mutants appeared normal (Fig. 5N). However, at E14.5 the altered morphology in the posterior palate of *36Pub* mutants was accompanied by a failure to posteriorly expand the *Tbx22* expression domain (Fig. 5P). Consistent with perturbed epithelial-mesenchymal signaling, we observed elevated and ectopic expression of the FGF-responsive genes *Etv5*, *Barx1*, and *Msx1* as well as the altered expression of *Tbx22* in regions of the *36Pub* mutant palate that normally express *Spry2*.

2.5. Loss of Spry2 alters Shh expression and signaling domains in the developing palate

SHH signaling plays a critical role in craniofacial development and disruption of this pathway can result in severe craniofacial defects including holoprosencephaly. During palate development the expression of *Shh* and that of its receptor *Patched1* (*Ptc1*) is restricted to regions of thickened oral epithelium and the immediately adjacent mesenchyme, respectively (Rice et al., 2006). These regions of epithelial thickening on the oral surface of the palatal shelves correspond to the developing rugae. Typically, 7 to 9 rugae are found on the oral surface of the palate at birth (Fig. 6F). Based on the signaling center activity of regions of thickened epithelium in other developmental contexts such as the apical ectodermal ridge (AER) of the limb bud and the enamel knot of the tooth, it has been proposed that the developing rugae may similarly function to coordinate patterning and morphogenesis of the palate (Rice et al., 2004). It has been demonstrated that *Shh* expression in the developing palate is dependent upon input from both the FGF and BMP signaling pathways, highlighting signaling interactions between a network of genes that guide craniofacial morphogenesis (Rice et al., 2004; Zhang et al., 2002). We were therefore interested in determining whether the altered FGF signaling thresholds in the *36Pub* mutant palate may also impact *Shh* expression.

We first confirmed that *Shh* expression on the oral surface of the palatal shelves is restricted to the developing rugae. We also noted an additional posterior domain of expression in the presumptive soft palate that is oriented orthogonal to bands of expression in the rugae (Fig. 6A). We observed that as palate development progresses the number of *Shh* expression bands increases, presumably due to the formation of additional rugae. Remarkably, careful analysis of a group of incrementally staged wildtype embryos highlights a region in the mid palate medial to the molar tooth bud that appears to define the location of new rugae formation (Fig. 6A). Using the molar tooth bud and the first formed stripe of *Shh* expression as constant reference points it can be seen that the periodic formation of new rugae occurs just anterior to the first formed stripe. *Shh* expression in the more anterior rugae is robust and constant, however, expression medial to the tooth bud appears to gradually increase and then separate into two bands that then become distinct stripes of expression. The region of rugae formation is initially positioned in the anterior half of the palate at E11.5. However, the elaboration of nascent rugae occurring in a generally anterior direction results in the apparent posterior regression of this region of the palate (compare position of red asterisks in Fig 6A). This implies that rostral extension of the anterior palate is accomplished at least in part through recruitment of cells from this more posterior region of the palate.

We next examined the expression of *Shh* and its receptor *Ptc1* at E14.5 in wildtype and *36Pub* mutant palates. Compared to the tightly organized bands of *Shh* seen in the wildtype palate, *Shh* expression in the mutant palate is defuse and fragmented into disorganized clumps of expressing cells (Fig. 6B&C). To determine whether the loss of *Spry2* also impacts other components of SHH signaling we examined the expression of *Ptc1* as a downstream target of *Shh*. In E14.5 wildtype palates, expression of *Ptc1* is restricted to the mesenchyme immediately adjacent to the developing rugae but is more broadly expressed throughout the mesenchyme of the presumptive soft palate (Fig. 6D). *Ptc1* expression in E14.5 *36Pub* mutant palates is no longer closely associated with the developing rugae and is highly disorganized with ectopic expression in broad domains of the palate (Fig. 6E). The loss of localized expression of *Ptc1* in the *36Pub* mutant palate suggests that spatially restricted SHH signaling is impacted. Interestingly, *Ptc1* expression underlying the first formed stripe of *Shh* expression appears to be less impacted than subsequently formed rugae domains. As evidence of the impact of altered *Shh* expression during palate development, we observed that at E18.5 rugae morphology is severely disrupted in the cleft palates of both *36Pub* homozygous and 36*Pub*/ $Spry^{2\Delta ORF}$ compound mutants when compared to the orderly array of rugae seen in wildtype littermates (Fig. 6 F&G and data not shown). This data supports a model where SHH signaling from the rugae is required for correct patterning and growth of the palate and that the proper establishment and or maintenance of *Shh* expression in the palate is dependent on appropriate FGF signaling thresholds. Taken together, these data reveal a novel segmental organization and previously unappreciated dynamic underlying the growth and patterning of the developing palate.

2.6. Altered cellular responses in the Spry2-deficient palate

We next investigated whether morphogenic cellular responses such as proliferation, apoptosis or differentiation were altered in the *36Pub* mutant. Typically, models of cleft palate where the shelves fail to make midline contact document diminished growth marked by reduced proliferation or increased cell death. We examined *36Pub* mutant palates for changes in cell death as detected by Nile blue sulfate staining and TUNEL assay. Cell death appeared unaltered throughout the E14.5 mutant palate (data not shown). Cellular proliferation assayed by BrdU incorporation however, did reveal that the mitotic index in the E14.5 *36Pub* mutant palate was increased. Elevated proliferation was observed in both the epithelium and mesenchyme with the most significant increase evident in the mid to posterior palate, consistent with the regions showing altered morphological progression (Fig. 7 and Supplementary Table 1). Additionally, we measured cell proliferation at E13.5 and E15.5 and observed regionally elevated mitotic indices in the *36Pub* mutant palate at these time points as well. Interestingly, the increased proliferation within the mutant palate relative to wildtype appears to involve both a temporal and spatial dynamic (Supplementary Table 1). While increased proliferation is not commonly recognized as a mechanistic basis for failed palatal development, such altered proliferation could lead to dysregulated growth and loss of coordinated progression of shelf morphology. The failure to acquire the correct shape at the appropriate time with respect to the overall growth of the face and oral cavity therefore represents a temporal dysmorphology in orofacial development that results in the failed midline contact of the palatal shelves.

The morphogenic movements of shelf reorientation and closure occur concurrently with cellular differentiation that gives rise to the palatal processes of the maxilla and palatine bones of the hard palate. Interestingly, analysis of skeletal preparations of E18.5 wildtype, 36*Pub*−/−;*Spry2*-BAC-69 transgenic embryos revealed a reduced size and altered morphology of the palatal processes of the maxilla and palatine bones in the transgenic animals, whereas in the 36*Pub*−/− mutant these bones are vestigial and absent, respectively (Fig. 8A-C). In the wildtype palate, mesenchymal condensation and intramembranous ossification begins around E14.0. We compared skeletogenic differentiation of wildtype and mutant palates between E14.5 and E15.5. In E14.5 wildtype embryos mesenchymal condensations are present in the osteogenic compartment along the anterior-posterior length of the maxilla. By E15.5 these condensations extend into the fused palatal shelves and show signs of significant matrix deposition (see Fig. 1A,B,C & I,J,K). We found very little histological evidence of these mesenchymal condensations within the osteogenic compartments of the *36Pub* mutant maxilla at E14.5 (see Fig. 1E,F,&G). The extent of ossification in E15.5 *36Pub* mutants was greatly reduced when compared to stage matched wildtype embryos (compare Fig. 1 I-K with M-O). We also noted that the degree of skeletal differentiation along the anterior-posterior axis in mutants appeared particularly reduced in the middle and posterior palate (compare Fig. 1I & 1M with Fig. 1K & 1O). This region corresponds to the area of the palate that would normally give rise to the maxillary and palatine processes. Thus, the development of the *36Pub* mutant palatal shelves does not appear to be completely arrested. Rather, their morphological and differentiative progression appears to be retarded with the posterior half of the palate being most severely impacted.

3. Discussion

The formation of the face and palate is dependent on the highly coordinated outgrowth, movement and fusion of paired facial primordia and palatal shelves. These morphogenic steps are under the control of reciprocal signaling interactions between adjacent epithelia and mesenchyme that involve the integration of the FGF, BMP, and SHH pathways. In this study we have shown that the FGF antagonist *Spry2* plays a role in craniofacial development. We investigated *Spry2* as a gene required for normal palatogenesis based on its activity as a modulator of FGF/RTK signaling and expression in the developing palate. Morphogenesis and skeletal differentiation of the palate is disrupted in mice homozygous for the *36Pub* deletion that removes the *Spry2* locus. Furthermore, a targeted mutation of *Spry2* fails to complement the *36Pub* deletion cleft palate phenotype. Interestingly, mice homozygous for the $Spry^{2\Delta \mathrm{ORF}}$ mutation do not display cleft palate. Differences in genetic background potentially provide a basis for this discrepancy. The *36Pub* deletion and $Spry^{2\Delta \mathrm{ORF}}$ mice used in this study are at N12 and N7 generations on a C57BL/6J genetic background, respectively. Additional studies will also be needed to determine whether the loss of another gene or genomic feature within the cleft palate critical interval sensitize the *36Pub* mutant mice to the loss of *Spry2* function and thereby contribute to the cleft palate phenotype. We also show that a *Spry2*-BAC transgene rescues craniofacial defects associated with the *36Pub* deletion mutant in a dosage dependent manner. Consistent with the loss of SPRY2 antagonism of FGF signaling the *36Pub* deletion mutant palates showed excessive proliferation along with elevated, ectopic expression of FGF-responsive genes. This study presents data that highlight a role for *Spry2* in the regulation of complex dosage dependent signaling interactions controlling orofacial development.

3.1. Palate morphogenesis relies on growth factor signaling thresholds that are modulated by Spry2 to coordinate regional cell proliferation, patterning, and differentiation

Mutations in a number of genes disrupt various and distinct aspects of palatal development. As a first example, clefting in *Tgfβ3* and *Egfr* mutants results from defective fusion of the palatal shelves. Although *Spry2* also acts to modulate EGF signaling, the defect in the *Spry2* deficient palate is manifest at earlier stages when FGF signaling has been shown to be critical for palate morphogenesis (Miettinen et al., 1999; Proetzel et al., 1995; Rice et al., 2004). Mutations disrupting *Msx1* provide a second example where clefting is a result of reduced proliferation and arrested shelf outgrowth (Satokata and Maas, 1994; Zhang et al., 2002). Our analysis of loss of *Spry2* function highlights a third mechanism for cleft palate where increased proliferation results in discoordination of palate growth and the morphogenic movements necessary for midline contact.

Our findings are consistent with increasing evidence that outgrowth and patterning is differentially regulated along the anterior-posterior axis of the palate and is achieved through regional differences in epithelial-mesenchymal signaling competence (Hilliard et al., 2005). The expanded and ectopic expression of *Msx1* and *Barx1* expression in *Spry2*-deficient embryos indicates that anterior-posterior patterning is altered. The reduced skeletal differentiation in more posterior skeletal elements potentially reflects the impact of this altered A-P patterning. The highest levels of *Barx1* expression in the posterior palatal mesenchyme becomes progressively restricted to the non-osteogenic soft palate. Further studies will be needed to investigate whether the ectopic and elevated *Barx1* expression in *Spry2*-deficient palates could interfere with osteoblastogenesis. One possibility is an alteration of WNT signaling shown to be important for osteoblast lineage development (Day et al., 2005). Targeted disruption of *Barx1* has revealed its importance in the regulation of the WNT signaling antagonists *sFrp1* and *sFrp2* (Kim et al., 2005). Importantly, inhibition of canonical Wnt-β-catenin signaling has also been proposed to be critical for the differentiation of bipotential osteo-chondroprogenitor cells (Hartmann, 2006).

The failure to upregulate *Tbx22* in the posterior palate at E14.5 may also be the result of altered patterning of the *Spry2*-deficient palate. It is interesting to note that putative *Msx1* binding sites in conserved sequences of the 5′ regulatory region of *Tbx22* have been identified and that *Msx1* is typically considered to act as a transcriptional repressor (Herr et al., 2003). The ectopic expression of *Msx1* in the mid-posterior palate in a domain that overlaps the normal domain of *Tbx22* expression may explain the failure to upregulate *Tbx22* at E14.5. Data from a targeted knock out of *Tbx22* as to the function of this gene during palate development has not yet been reported. This study presents evidence that suggests *Tbx22* is required for the normal growth of the posterior palate. Our data support a model where *Spry2*-mediated modulation of signal strength plays a key role in establishing thresholds that correspond with differential FGF signaling responsiveness important for patterning the anterior-posterior axis of the palate.

3.2. Spry2 as part of a signaling network that guides palate and facial development

Our results provide insight into FGF pathway control of tissue interactions involved in craniofacial development. Cellular proliferation during palate development has been shown to depend on multiple signaling pathways. Reciprocal epithelial-mesenchymal communication integrates this spatially distributed signaling activity into a network of interactions that coordinate the morphogenesis of the palate (Fig. 9). A mesenchymal *Bmp4/Msx1* feedback loop is required for *Shh* expression leading to proliferation in the anterior palate (Zhang et al., 2002). Mesenchymal *Fgf10* signaling through *Fgfr2b* has also been shown to regulate *Shh* expression and cell proliferation, particularly in the epithelium. The loss of normal expression of *Shh* and its receptor *Ptc1* in the *Spry2* deficient palate underscores the importance of maintaining appropriate levels of FGF signaling input to this network. Furthermore, the localized and dynamic expression of *Shh* suggest that the developing rugae act as signaling centers where the FGF, BMP and SHH pathways are integrated to form a network that controls palatal growth. Evidence supporting our model that *Shh* expression and new rugae formation represent landmarks for the organization of signaling interactions that direct the rostral extension of the palate comes from recent work by Li and Ding (Li and Ding, 2007). Based upon the expansion of the anteriorly restricted *Shox-2* and regression of the posteriorly restricted *Meox-2* expression domains from E12.5 to E14.5 without an accompanying regional difference in proliferation, the authors hypothesize that the expansion of the anterior palate involves recruitment of once posterior *Meox-2* expressing cells and their conversion into anterior *Shox-2* expressing cells.

Loss of the inhibitor *Spry2* results in expanded expression of FGF responsive genes in both the epithelium and mesenchyme, increased proliferation in both the epithelium and mesenchyme, and altered morphodifferentiative progression of palate growth. Notably, *Etv5* and *Barx1* expression is expanded in the anterior epithelium adjacent to *Fgf10* expressing mesenchyme and the expression of *Barx1* and *Msx1* is expanded and ectopic in the mesenchyme of *Spry2*-deficient mutants. These results strongly implicate a role for *Spry2* inhibition of FGF signaling in both the epithelium and mesenchyme. A reciprocal source of FGF in palatal epithelium regulating mesenchymal proliferation has not been reported. However, based upon spatial gene expression and the 40% incidence of cleft palate in loss of function mouse mutants, *Fgf9* is a strong candidate as an epithelial FGF signaling source in the palate (Colvin et al., 1999; Colvin et al., 2001). *Fgf9* has been shown to be able to induce expression of *Msx1* in oral mesenchyme during odontogenesis (Kettunen and Thesleff, 1998). It is therefore possible that the ectopic and expanded *Msx1* expression in the *Spry2*-deficient palate is a result of the loss of antagonism leading to unregulated *Fgf9* signaling through its high affinity receptor *Fgfr2c* in the mesenchyme (Ornitz et al., 1996) (Fig. 9). In support of this hypothesis Klein et al. report that the loss of *Spry2* antagonism during tooth development leads to ectopic expression of FGF target genes in tissue that is normally refractory to this signaling input and that this defect can be fully rescued by genetically reducing *Fgfr2* dosage (Klein et al., 2006). Additionally, an engineered gain of function mutation in *Fgfr2c* phenocopies the craniofacial defects of Crouzon and Pfeiffer syndromes and results in cleft palate and altered skeletal differentiation (Eswarakumar et al., 2004; Ibrahimi et al., 2004). This activating mutation provides an analogous model to the loss of *Spry2* antagonism. Both the *Fgfr2c* gain of function and *Spry2* loss of function reflect the resulting impact of altered FGF signaling strength on craniofacial development. Taken together, our data support a model where reciprocal tissue interactions involving FGF signaling controls proliferation, patterning, and the necessary shape changes required to close the palate utilizing different epithelial and mesenchymal FGF signaling effectors and a common antagonist, *Spry2*.

3.3. FGF signaling and the genetic basis of craniofacial malformations

Orofacial anomalies are among the most prominent class of birth defects, occurring in ~1/500 to 1/2,500 births. The rapid proliferative expansion of the facial primordia and the need to coordinate the overlapping processes of complex morphogenic movements with cellular differentiation are defining features of the sensitivity of craniofacial development to disruption by genetic and environmental insult. Genetic analysis of human patients affected by craniofacial syndromes as well as gene perturbations in mouse has generated a great deal of insight into the genes involved in craniofacial development. Mutations leading to orofacial clefting can be categorized as either syndromic or nonsyndromic depending on the presence or absence of additional developmental anomalies (Jugessur and Murray, 2005). That a significant majority of cleft lip and palate defects appear to be nonsyndromic underscores the molecular and genetic complexity of the underlying developmental program. Precise and efficient communication between adjacent cell layers is a prerequisite for the ordered progression of such a program. Therefore, progress in the prevention of orofacial clefting will require not only the identification of additional genes, but also the placement of the various components into molecular pathways and interacting networks. Genetic network models will provide a framework for studying how various mutations and allelic combinations together with environmental factors impact the morphogenetic events required for normal orofacial development. The data presented here identify *Spry2* as a key component of this network, acting to modulate FGF signaling strength and defining regional responsiveness to epithelial-mesenchymal signaling interactions that direct the outgrowth and patterning of the palatal shelves.

Identifying *Spry2* as a gene critical for palate development provides further insight as to how altered FGF signaling contributes to craniofacial malformations and will help make this class of birth defects more genetically tractable. Further support for a role of *Spry2* during palate development comes from medical sequence analysis of patients with cleft palate accompanied by a familial history of cleft palate. In a recent report Vieira and coworkers identified mutations of *Spry2* in nucleotides that are conserved from *Xenopus* to human that along with mutations identified in 5 other genes may collectively account for as much as 6% of nonsyndromic clefting (Vieira et al., 2005). The dosage-dependent role of *Spry2* also provides insight into the extent to which developmental processes can tolerate signaling perturbations. Mice carrying a deletion of *Spry2* on an inbred C57BL/6J background have a high probability of developing clefts of both the primary and secondary palate. However, restoring *Spry2* expression to ~25% normal levels is enough to rescue the palatal defects by shifting shelf growth into a window that is compatible with the overall timing of orofacial development. Our findings emphasize that developmental control is achieved by a network of interactions that elicit morphogenic responses that are sensitive to signaling thresholds. Thus, variations in the overall signaling balance can lead to differences in final form that range from unique facial characteristics to birth defects.

4. Experimental procedures

4.1. Mice and production of Spry2-BAC transgenics

36*Pub* deletion mice were maintained on a C57BL/6J genetic background (currently N12). *36Pub* mice were genotyped in a PCR assay using the deletion flanking markers *D14Mit265* and *D14Mit177* as previously described (Roix et al., 2001). $Spry2^{\Delta ORF}$ mice were genotyped as described (Shim et al., 2005).

The *Spry2*-BAC used for transgenic mouse production was isolated by PCR screening the CITB-CJ7 (129S1/Sv) BAC library (Research Genetics). The size of the BAC was determined by matching BAC-end sequences against the mouse genome (Ensembl MGSC v15.30.1) and pulse field gel electrophoresis analysis as previously described (Peterson et al., 2002). Gene content and conserved sequence features on the BAC were characterized using computational methods as previously described (Peterson et al., 2002). C57BL/6J *Spry2*-BAC transgenic animals were produced by pronuclear injection of purified BAC DNA. Transgenic animals were genotyped using a PCR assay based on the $(CA)_n$ repeat marker *D14J42* that detects the 129S1/Sv BAC-derived sequence in the C57BL/6J inbred genomic background. Southern blot analysis was used to determine a copy number of 1-2 integration events per genome with strictly Mendelian inheritance for the *Spry2*-BAC lines 2 and 69 used in this study (data not shown). All primer sequences are available upon request.

4.2. Histology and in situ hybridization

Embryos were obtained from timed matings with E0.5 defined as noon of the day of the vaginal plug. Tissue samples for histological analysis were dissected in cold PBS (phosphate buffered saline) and fixed overnight in either Bouin's fixative or 4% paraformaldehyde (PFA) and processed and stained with Hematoxylin and Eosin following standard protocols.

Samples for whole mount *in situ* hybridization analysis were dissected in cold PBS and immediately fixed in 4% PFA overnight at 4°C followed by several rinses of PBST (PBS with 0.1% Tween-20), dehydrated to 100% methanol and stored at −20°C. Palates were dissected free of surrounding tissue and processed intact or sectioned into 1-2 mm tissue slices using a microtome blade. A detailed *in situ* hybridization protocol is available upon request. In order to gain a qualitative assessment of relative expression levels all wildtype and mutant tissues were processed in a single vial and detected for an identical length of time.

The following genes were PCR amplified, T/A cloned (Invitrogen) and used to generate anti-sense riboprobes for the expression analyses: *Barx1* (nt 175-1334 of the coding sequence); *Etv5* (nt 1591-3245 of the coding sequence); *Fgf10* (nt 1-630 of the coding sequence); *Fgfr2* (nt 1427-2465 of the coding sequence); *Msx1* (nt 1-1213 of the coding sequence); *Ptc1* (nt 2903-4262 of the coding sequence); *Spry2* (nt 16-1465 of the coding sequence); *Shh* (full length cDNA clone from A. McMahon); Tbx22 (nt 307-1547 of the coding sequence).

4.3. Cell proliferation and survival assays

Cell proliferation was determined using a BrdU labeling kit (Roche) and cell death was determined by TUNEL analysis using an *in situ* cell death detection kit (Roche) according to the manufacturer's instructions. For BrdU incorporation pregnant females were injected with 20 μl/gram of body weight with 10 mM BrdU and embryos collected one hour later. Tissues were dissected in cold PBS, fixed overnight in 4% PFA at 4°C and embedded in paraffin. 10 μm serial frontal sections were collected at 6 sections per slide and grouped into four regions each representing one-fourth the total anterior to posterior length of the individual palate (anterior, mid-anterior, mid-posterior, and posterior). Serial sets of slides from each region were processed for BrdU labeling and TUNEL analysis. Nuclei were counterstained with DAPI. Mitotic index and cellularity data were obtained by counting the number of labeled cells and total number of cells per unit area in an identical region of the palatal shelf. Statistical analysis was performed using ANOVA and student's t-test. Embryos for Nile Blue Sulfate (NBS) staining were dissected and rinsed in cold PBS and then incubated in filtered 10 mg/ml of NBS in PBS with 0.1% Tween-20 for 45 minutes at 37°C.

4.4. RNA extraction and Quantitative RT-PCR analysis

E14.5 palatal tissue was dissected from surrounding tissue, snap frozen in 200 μl of RNAlater (Ambion) and stored at −80°C. Total RNA was extracted using TRIzol reagent (Invitrogen) according to the manufacturer's instructions. RNA was DNase I treated (Ambion) and RNA quantity and quality was checked using an Agilent Bioanalyzer 2100. 1 μg of total RNA was primed using random hexamers and reverse transcribed using Superscript II reverse transcriptase (Invitrogen) and diluted 1:10 prior to PCR analysis.

Relative quantification of expression levels for *Spry2* in the palate were assayed in E14.5 wildtype, *36Pub* mutant, and *Spry2*-BAC hemizygous line 2 and line 69 *36Pub* mutant samples. Four samples of each genotype were run in triplicate and β–actin expression was used to normalize relative expression levels. Real-time PCR was performed on an ABI 7500 using the following TaqMan gene expression assays: *Spry2* Mm00442344_m1; mouse ACTB 4352341E in a 20 μl reaction solution containing TaqMan univesral mastermix with UNG (Applied Biosystems) and 5 ng of cDNA. Data were analyzed as described (Peirson et al., 2003). Cycling conditions were 50 °C for 2 minutes, 95°C for 10 minutes followed by 95°C for 15 seconds and 60°C for 1 minute for 40 cycles.

Supplementary Material

Refer to Web version on PubMed Central for supplementary material.

Acknowledgments

We thank Drs. Susan Ackerman and Tom Gridley for valuable discussions and comments on the manuscript. We thank Dr. Gail Martin for providing *Spry*$^{2\Delta}$ORF mice. We thank Kevin Peterson for help with genomic analysis and Jim Hagarman for excellent technical assistance. This work was supported by NIH grants HD36434 and HD41066 (T.P.O.).

References

Alappat S, Zhang ZY, Chen YP. Msx homeobox gene family and craniofacial development. Cell Res 2003;13:429–42. [PubMed: 14728799]

Alappat SR, Zhang Z, Suzuki K, Zhang X, Liu H, Jiang R, Yamada G, Chen Y. The cellular and molecular etiology of the cleft secondary palate in Fgf10 mutant mice. Dev Biol 2005;277:102–13. [PubMed: 15572143]

Bachler M, Neubuser A. Expression of members of the Fgf family and their receptors during midfacial development. Mech Dev 2001;100:313–6. [PubMed: 11165488]

Barlow AJ, Bogardi JP, Ladher R, Francis-West PH. Expression of chick Barx-1 and its differential regulation by FGF-8 and BMP signaling in the maxillary primordia. Dev Dyn 1999;214:291–302. [PubMed: 10213385]

Basson MA, Akbulut S, Watson-Johnson J, Simon R, Carroll TJ, Shakya R, Gross I, Martin GR, Lufkin T, McMahon AP, Wilson PD, Costantini FD, Mason IJ, Licht JD. Sprouty1 is a critical regulator of GDNF/RET-mediated kidney induction. Dev Cell 2005;8:229–39. [PubMed: 15691764]

Bei M, Maas R. FGFs and BMP4 induce both Msx1-independent and Msx1-dependent signaling pathways in early tooth development. Development 1998;125:4325–33. [PubMed: 9753686]

Chou MJ, Kosazuma T, Takigawa T, Yamada S, Takahara S, Shiota K. Palatal shelf movement during palatogenesis: a fate map of the fetal mouse palate cultured in vitro. Anat Embryol (Berl) 2004;208:19–25. [PubMed: 14986130]

Colvin JS, Feldman B, Nadeau JH, Goldfarb M, Ornitz DM. Genomic organization and embryonic expression of the mouse fibroblast growth factor 9 gene. Dev Dyn 1999;216:72–88. [PubMed: 10474167]

Colvin JS, White AC, Pratt SJ, Ornitz DM. Lung hypoplasia and neonatal death in Fgf9-null mice identify this gene as an essential regulator of lung mesenchyme. Development 2001;128:2095–106. [PubMed: 11493531]

Day TF, Guo X, Garrett-Beal L, Yang Y. Wnt/beta-catenin signaling in mesenchymal progenitors controls osteoblast and chondrocyte differentiation during vertebrate skeletogenesis. Dev Cell 2005;8:739–50. [PubMed: 15866164]

De Moerlooze L, Spencer-Dene B, Revest J, Hajihosseini M, Rosewell I, Dickson C. An important role for the IIIb isoform of fibroblast growth factor receptor 2 (FGFR2) in mesenchymal-epithelial signalling during mouse organogenesis. Development 2000;127:483–92. [PubMed: 10631169]

Eswarakumar VP, Horowitz MC, Locklin R, Morriss-Kay GM, Lonai P. A gain-of-function mutation of Fgfr2c demonstrates the roles of this receptor variant in osteogenesis. Proc Natl Acad Sci U S A 2004;101:12555–60. [PubMed: 15316116]

Eswarakumar VP, Monsonego-Ornan E, Pines M, Antonopoulou I, Morriss-Kay GM, Lonai P. The IIIc alternative of Fgfr2 is a positive regulator of bone formation. Development 2002;129:3783–93. [PubMed: 12135917]

Ferguson MW. Palate development. Development 1988;103(Suppl):41–60. [PubMed: 3074914]

Firnberg N, Neubuser A. FGF signaling regulates expression of Tbx2, Erm, Pea3, and Pax3 in the early nasal region. Dev Biol 2002;247:237–50. [PubMed: 12086464]

Francis-West P, Ladher R, Barlow A, Graveson A. Signalling interactions during facial development. Mech Dev 1998;75:3–28. [PubMed: 9739099]

Hacohen N, Kramer S, Sutherland D, Hiromi Y, Krasnow MA. sprouty encodes a novel antagonist of FGF signaling that patterns apical branching of the Drosophila airways. Cell 1998;92:253–63. [PubMed: 9458049]

Hansen J, Floss T, Van Sloun P, Fuchtbauer EM, Vauti F, Arnold HH, Schnutgen F, Wurst W, von Melchner H, Ruiz P. A large-scale, gene-driven mutagenesis approach for the functional analysis of the mouse genome. Proc Natl Acad Sci U S A 2003;100:9918–22. [PubMed: 12904583]

Hartmann C. A Wnt canon orchestrating osteoblastogenesis. Trends Cell Biol 2006;16:151–8. [PubMed: 16466918]

Herr A, Meunier D, Muller I, Rump A, Fundele R, Ropers HH, Nuber UA. Expression of mouse Tbx22 supports its role in palatogenesis and glossogenesis. Dev Dyn 2003;226:579–86. [PubMed: 12666195]

Hilliard SA, Yu L, Gu S, Zhang Z, Chen YP. Regional regulation of palatal growth and patterning along the anterior-posterior axis in mice. J Anat 2005;207:655–67. [PubMed: 16313398]

Ibrahimi OA, Zhang F, Eliseenkova AV, Itoh N, Linhardt RJ, Mohammadi M. Biochemical analysis of pathogenic ligand-dependent FGFR2 mutations suggests distinct pathophysiological mechanisms for craniofacial and limb abnormalities. Hum Mol Genet 2004;13:2313–24. [PubMed: 15282208]

Jugessur A, Murray JC. Orofacial clefting: recent insights into a complex trait. Curr Opin Genet Dev 2005;15:270–8. [PubMed: 15917202]

Kettunen P, Thesleff I. Expression and function of FGFs-4, -8, and -9 suggest functional redundancy and repetitive use as epithelial signals during tooth morphogenesis. Dev Dyn 1998;211:256–68. [PubMed: 9520113]

Kim BM, Buchner G, Miletich I, Sharpe PT, Shivdasani RA. The stomach mesenchymal transcription factor Barx1 specifies gastric epithelial identity through inhibition of transient Wnt signaling. Dev Cell 2005;8:611–22. [PubMed: 15809042]

Kim HJ, Rice DP, Kettunen PJ, Thesleff I. FGF-, BMP- and Shh-mediated signalling pathways in the regulation of cranial suture morphogenesis and calvarial bone development. Development 1998;125:1241–51. [PubMed: 9477322]

Klein OD, Minowada G, Peterkova R, Kangas A, Yu BD, Lesot H, Peterka M, Jernvall J, Martin GR. Sprouty Genes Control Diastema Tooth Development via Bidirectional Antagonism of Epithelial-Mesenchymal FGF Signaling. Dev Cell 2006;11:181–190. [PubMed: 16890158]

Li Q, Ding J. Gene expression analysis reveals that formation of the mouse anterior secondary palate involves recruitment of cells from the posterior side. Int J Dev Biol 2007;51:167–72. [PubMed: 17294368]

Liu Z, Xu J, Colvin JS, Ornitz DM. Coordination of chondrogenesis and osteogenesis by fibroblast growth factor 18. Genes Dev 2002;16:859–69. [PubMed: 11937493]

Marcano AC, Doudney K, Braybrook C, Squires R, Patton MA, Lees MM, Richieri-Costa A, Lidral AC, Murray JC, Moore GE, Stanier P. TBX22 mutations are a frequent cause of cleft palate. J Med Genet 2004;41:68–74. [PubMed: 14729838]

Miettinen PJ, Chin JR, Shum L, Slavkin HC, Shuler CF, Derynck R, Werb Z. Epidermal growth factor receptor function is necessary for normal craniofacial development and palate closure. Nat Genet 1999;22:69–73. [PubMed: 10319864]

Min H, Danilenko DM, Scully SA, Bolon B, Ring BD, Tarpley JE, DeRose M, Simonet WS. Fgf-10 is required for both limb and lung development and exhibits striking functional similarity to Drosophila branchless. Genes Dev 1998;12:3156–61. [PubMed: 9784490]

Minowada G, Jarvis LA, Chi CL, Neubuser A, Sun X, Hacohen N, Krasnow MA, Martin GR. Vertebrate Sprouty genes are induced by FGF signaling and can cause chondrodysplasia when overexpressed. Development 1999;126:4465–4475. [PubMed: 10498682]

Ornitz DM, Xu J, Colvin JS, McEwen DG, MacArthur CA, Coulier F, Gao G, Goldfarb M. Receptor specificity of the fibroblast growth factor family. J Biol Chem 1996;271:15292–7. [PubMed: 8663044]

Peirson SN, Butler JN, Foster RG. Experimental validation of novel and conventional approaches to quantitative real-time PCR data analysis. Nucleic Acids Res 2003;31:e73. [PubMed: 12853650]

Peterson KA, King BL, Hagge-Greenberg A, Roix JJ, Bult CJ, O'Brien TP. Functional and comparative genomic analysis of the piebald deletion region of mouse chromosome 14. Genomics 2002;80:172–84. [PubMed: 12160731]

Proetzel G, Pawlowski SA, Wiles MV, Yin M, Boivin GP, Howles PN, Ding J, Ferguson MW, Doetschman T. Transforming growth factor-beta 3 is required for secondary palate fusion. Nat Genet 1995;11:409–14. [PubMed: 7493021]

Revest JM, Spencer-Dene B, Kerr K, De Moerlooze L, Rosewell I, Dickson C. Fibroblast growth factor receptor 2-IIIb acts upstream of Shh and Fgf4 and is required for limb bud maintenance but not for the induction of Fgf8, Fgf10, Msx1, or Bmp4. Dev Biol 2001;231:47–62. [PubMed: 11180951]

Rice R, Connor E, Rice DP. Expression patterns of Hedgehog signalling pathway members during mouse palate development. Gene Expr Patterns 2006;6:206–12. [PubMed: 16168717]

Rice R, Spencer-Dene B, Connor EC, Gritli-Linde A, McMahon AP, Dickson C, Thesleff I, Rice DP. Disruption of Fgf10/Fgfr2b-coordinated epithelial-mesenchymal interactions causes cleft palate. J Clin Invest 2004;113:1692–700. [PubMed: 15199404]

Rice R, Thesleff I, Rice DP. Regulation of Twist, Snail, and Id1 is conserved between the developing murine palate and tooth. Dev Dyn 2005;234:28–35. [PubMed: 16028273]

Roix JJ, Hagge-Greenberg A, Bissonnette DM, Rodick S, Russell LB, O'Brien TP. Molecular and functional mapping of the piebald deletion complex on mouse chromosome 14. Genetics 2001;157:803–15. [PubMed: 11156998]

Sakamoto MK, Nakamura K, Handa J, Kihara T, Tanimura T. Morphogenesis of the secondary palate in mouse embryos with special reference to the development of rugae. Anat Rec 1989;223:299–310. [PubMed: 2923281]

Satokata I, Maas R. Msx1 deficient mice exhibit cleft palate and abnormalities of craniofacial and tooth development. Nat Genet 1994;6:348–56. [PubMed: 7914451]

Sharrocks AD. The ETS-domain transcription factor family. Nat Rev Mol Cell Biol 2001;2:827–37. [PubMed: 11715049]

Shigetani Y, Nobusada Y, Kuratani S. Ectodermally derived FGF8 defines the maxillomandibular region in the early chick embryo: epithelial-mesenchymal interactions in the specification of the craniofacial ectomesenchyme. Dev Biol 2000;228:73–85. [PubMed: 11087627]

Shim K, Minowada G, Coling DE, Martin GR. Sprouty2, a mouse deafness gene, regulates cell fate decisions in the auditory sensory epithelium by antagonizing FGF signaling. Dev Cell 2005;8:553–64. [PubMed: 15809037]

Taketomi T, Yoshiga D, Taniguchi K, Kobayashi T, Nonami A, Kato R, Sasaki M, Sasaki A, Ishibashi H, Moriyama M, Nakamura K, Nishimura J, Yoshimura A. Loss of mammalian Sprouty2 leads to enteric neuronal hyperplasia and esophageal achalasia. Nat Neurosci 2005;8:855–7. [PubMed: 15937482]

Taniguchi K, Ayada T, Ichiyama K, Kohno R, Yonemitsu Y, Minami Y, Kikuchi A, Maehara Y, Yoshimura A. Sprouty2 and Sprouty4 are essential for embryonic morphogenesis and regulation of FGF signaling. Biochem Biophys Res Commun 2007;352:896–902. [PubMed: 17156747]

Thisse B, Thisse C. Functions and regulations of fibroblast growth factor signaling during embryonic development. Dev Biol 2005;287:390–402. [PubMed: 16216232]

Trokovic N, Trokovic R, Mai P, Partanen J. Fgfr1 regulates patterning of the pharyngeal region. Genes Dev 2003;17:141–53. [PubMed: 12514106]

Trumpp A, Depew MJ, Rubenstein JL, Bishop JM, Martin GR. Cre-mediated gene inactivation demonstrates that FGF8 is required for cell survival and patterning of the first branchial arch. Genes Dev 1999;13:3136–48. [PubMed: 10601039]

Tucker AS, Al Khamis A, Sharpe PT. Interactions between Bmp-4 and Msx-1 act to restrict gene expression to odontogenic mesenchyme. Dev Dyn 1998a;212:533–9. [PubMed: 9707326]

Tucker AS, Matthews KL, Sharpe PT. Transformation of tooth type induced by inhibition of BMP signaling. Science 1998b;282:1136–8. [PubMed: 9804553]

Vieira AR, Avila JR, Daack-Hirsch S, Dragan E, Felix TM, Rahimov F, Harrington J, Schultz RR, Watanabe Y, Johnson M, Fang J, O'Brien SE, Orioli IM, Castilla EE, Fitzpatrick DR, Jiang R, Marazita ML, Murray JC. Medical sequencing of candidate genes for nonsyndromic cleft lip and palate. PLoS Genet 2005;1:e64. [PubMed: 16327884]

NIH-PA Author Manuscript

NIH-PA Author Manuscript

Zhang Z, Song Y, Zhao X, Zhang X, Fermin C, Chen Y. Rescue of cleft palate in Msx1-deficient mice by transgenic Bmp4 reveals a network of BMP and Shh signaling in the regulation of mammalian palatogenesis. Development 2002;129:4135–46. [PubMed: 12163415]

NIH-PA Author Manuscript

NIH-PA Author Manuscript

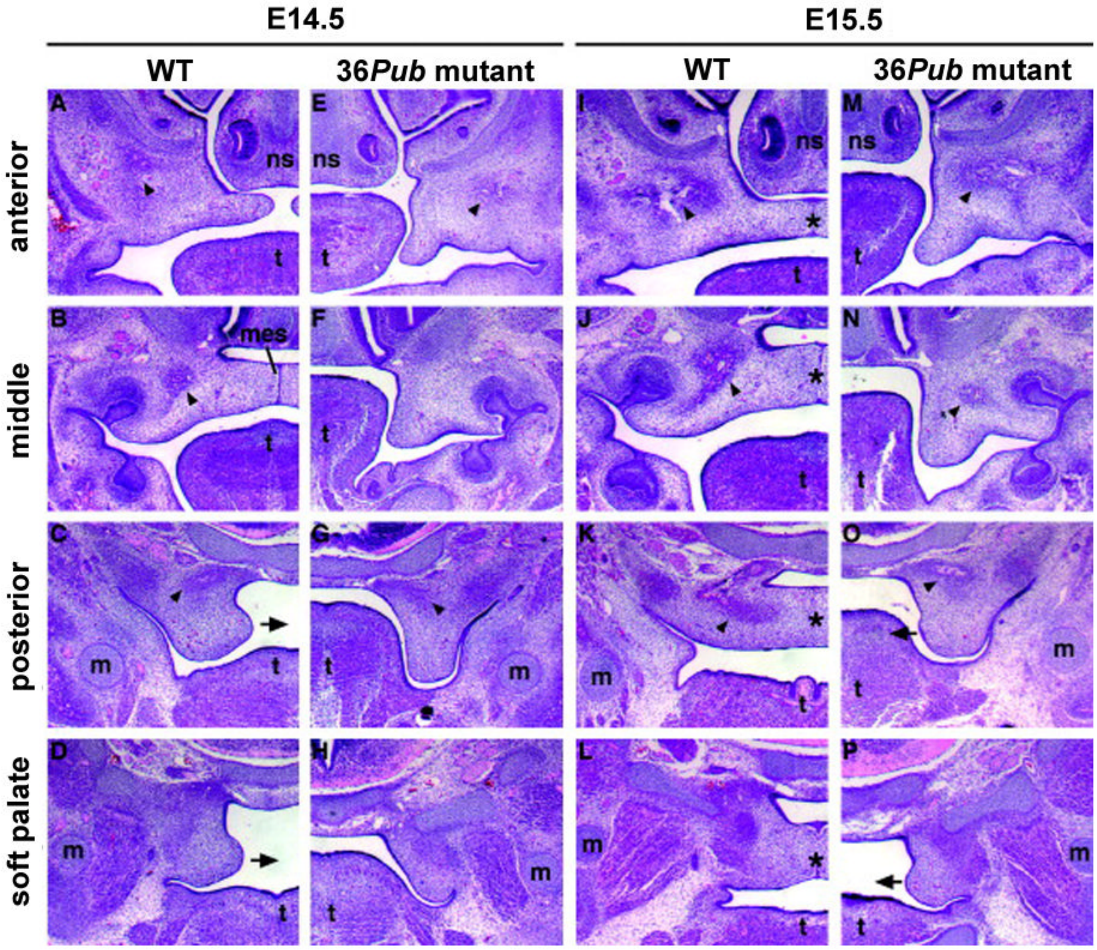

Fig. 1.

Altered morphogenic progression of the *36Pub* mutant palate. H&E stained serial frontal sections through the entire anterior-posterior length of E14.5 and E15.5 palates were grouped into four regions each representing one quarter of the total palatal length and the morphology of the palate within each region was compared between wildtype (E14.5 A-D; E15.5 I-L) and mutant (E14.5 E-H; E15.5 M-P). Images show the right side palatal shelf of the wildtype beside the contralateral mutant shelf from the same region for comparative purposes. By E14.5 the anterior palatal shelves (A) of the wildtype have elevated above the tongue and in the middle region (B) the shelves are in contact although still separated by the medial epithelial seam. The posterior palate (C) and region of the soft palate (D) of the E14.5 wildtype exhibit a medially projecting prominence indicative of directed growth towards the midline (black arrows). E14.5 *36Pub* mutant palates have not elevated in the anterior half (E, F) and the posterior palate (G) and region of the soft palate (H) have failed to acquire the shape changes associated with the transition from vertically- to medially-directed outgrowth. The E15.5 wildtype palate is closed along its entire A-P length (I-L) and fusion of the shelves by breakdown of the medial epithelial seam is nearly complete (asterisks). By E15.5 the *36Pub* mutant palate has still not elevated dorsal to the tongue (M,N) although the posterior half of the palate does exhibit limited growth towards the midline (arrows in O&P). Arrowheads point to sites of mesodermal condensation and matrix deposition associated with incipient intramembranous ossification that is particularly impacted in the middle and posterior of the mutant palate. Abbreviations: m, Meckel's cartilage; mes, medial epithelial seam; ns, nasal septum; t, tongue.

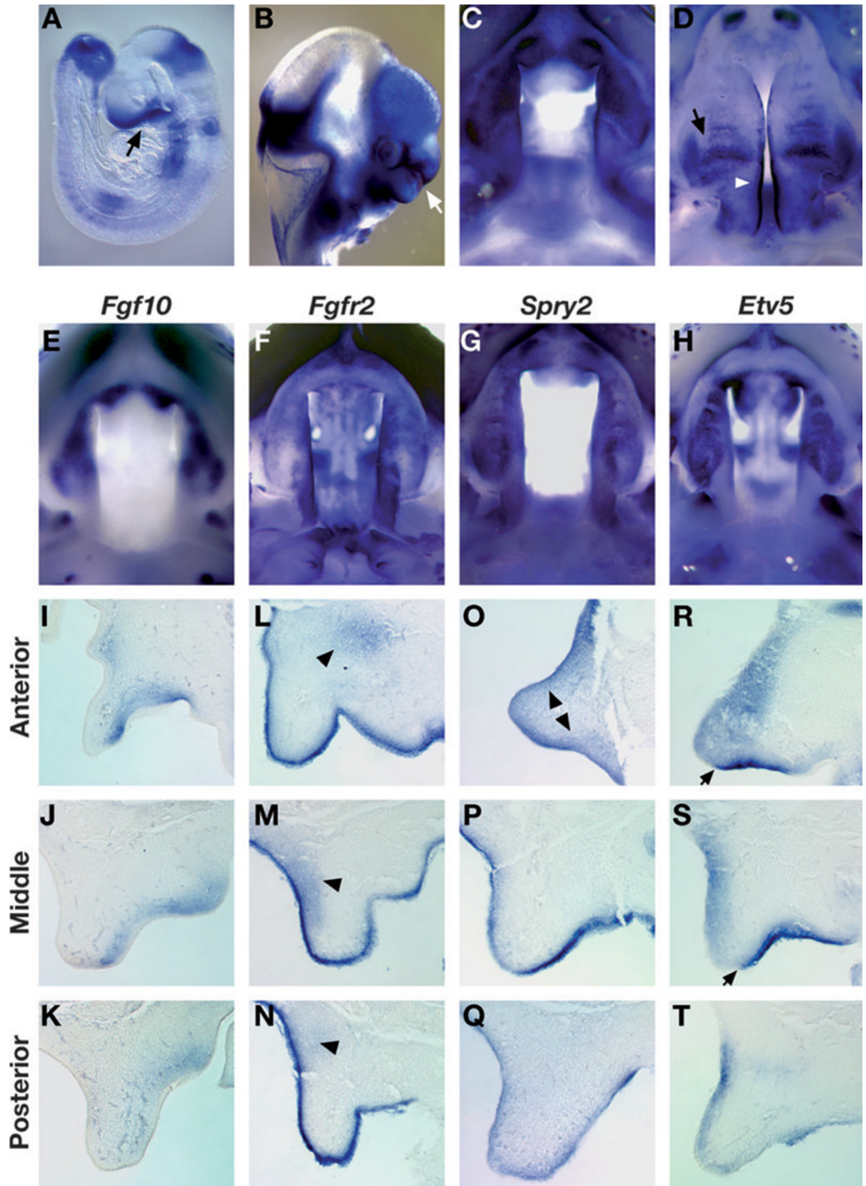

Fig. 2.

Spry2 expression during orofacial development. (A, B) *Spry2* is expressed in structures that will outgrow and fuse to form the primary palate and jaw. (A) At E9.5 *Spry2* is expressed in the telencephalon and olfactory placode as well as in both the maxillary and mandibular processes of the first branchial arch (arrow). By E11.5 (B) *Spry2* expression is seen in the area of fusion between the frontonasal process and the anterior maxillary process of the first branchial arch (white arrow). (C, D) Wholemount view of the oronasal cavity (rostrocaudal from top to bottom) showing dynamic expression of *Spry2* during palate development between E12.5 and E14.5. (C) At E12.5, *Spry2* is strongly expressed in the epithelium and mesenchyme of the anterior half of the oral cavity that is derived from the mid-maxilla of the first branchial arch. (D) Prior to contact of the shelves at E14.5 *Spry2* expression is seen in a broad domain in the mid-posterior palatal epithelium (arrow) and the along the medial aspect of the approaching shelves with strongest expression in the posterior half of the palate (white arrowhead). (E-H) Wholemount view of oronasal cavity (rostrocaudal from top to bottom) and (I-T) frontal section views of gene expression at E13.5 showing *Spry2* spatially referenced to the expression of components of the FGF signaling pathway (*Fgf10:* E, I, J, K; *Fgfr2*: F, L, M, N; *Spry2*: G, O, P, Q; *Etv5*: H, R, S, T). (E) *Fgf10* is expressed in the mesenchyme of the anterior two-thirds of the palate and becomes progressively localized to the oral side of the palatal shelf in the posterior region of its domain (I, J, & K). (F) *Fgfr2b* and *Fgfr2c* expression is detected with a single probe recognizing both isoforms. *Fgfr2b* is broadly expressed throughout the palatal epithelium (L, M, & N) whereas mesenchyme specific *Fgfr2c* is localized to discrete domains of osteogenic mesenchyme in the anterior maxilla and underlying the nasal epithelium (black arrowheads). (G,P) *Spry2* is expressed throughout the palatal epithelium with strongest levels on the oral side of the mid-palate. *Spry2* in the mesenchyme is strongly expressed in the anterior (O) and at slightly lower levels in the posterior (Q) with expression in the mid-palate tightly restricted to the mesenchyme subjacent to the nasal epithelium (P). (H) *Etv5* in the epithelium is restricted to the anterior two-thirds of the palate in the oral surface directly overlaying the *Fgf10* domain. *Etv5* in the mesenchyme is broadly expressed in the anterior palatal shelves (R), although more medially restricted than that of *Spry2* (compare O and R), and becomes progressively restricted to the mesenchyme subjacent to the nasal epithelium (S, T).

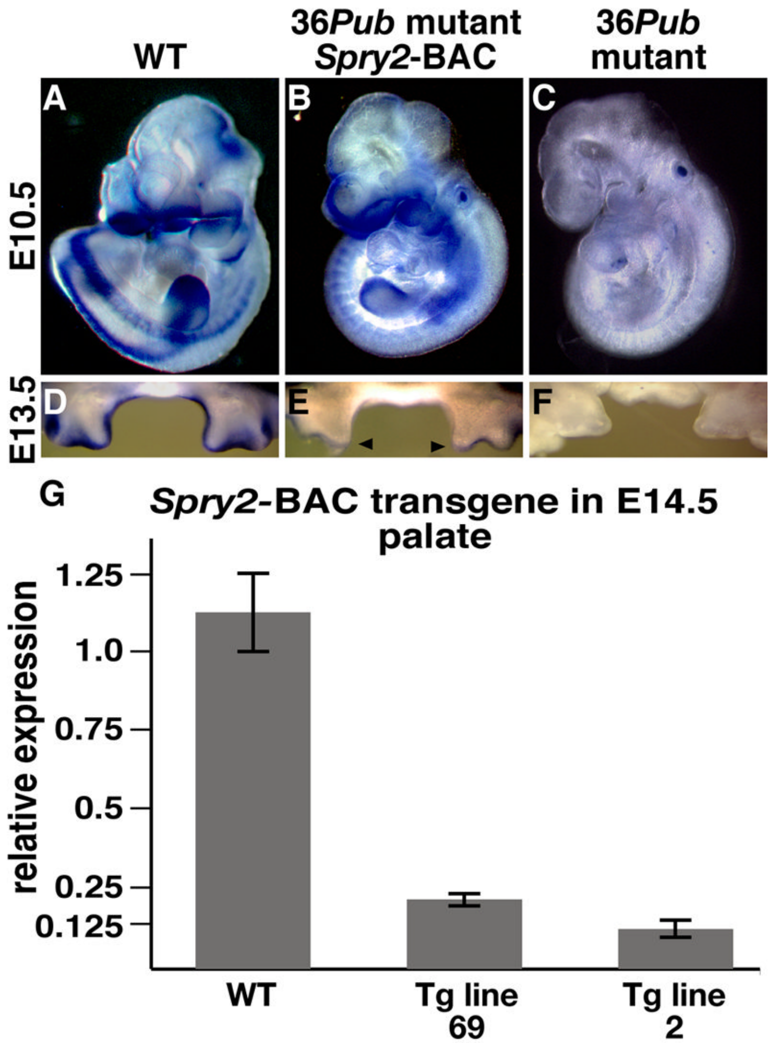

Fig. 3.

Spatial expression pattern from *Spry2*-BAC transgene is similar to endogenous *Spry2* expression but at reduced levels. (A-F) The *Spry2*-BAC drives expression in a pattern comparable to the endogenous locus. *Spry2* transcripts are detected in the developing branchial arches and facial primordia of wildtype embryos at E10.5 (A) and in a frontal view of E13.5 wildtype palatal shelves (D). The *Spry2*-BAC hemizygous, *36Pub* mutant shows comparable expression in the developing E10.5 embryo (B) as well as in the palatal shelves at E13.5 (E), note reduced expression levels (arrowheads). *Spry2* transcripts are absent in the non-transgenic *36Pub* mutant E10.5 embryo (C) and E13.5 palatal shelves (F). (G) Quantitative RT-PCR analysis of *Spry2* expression in *Spry2*-BAC transgenic line 2 and 69 using E14.5 palatal tissue shows *Spry2* is expressed at ~12.5% and ~25% of endogenous levels, respectively.

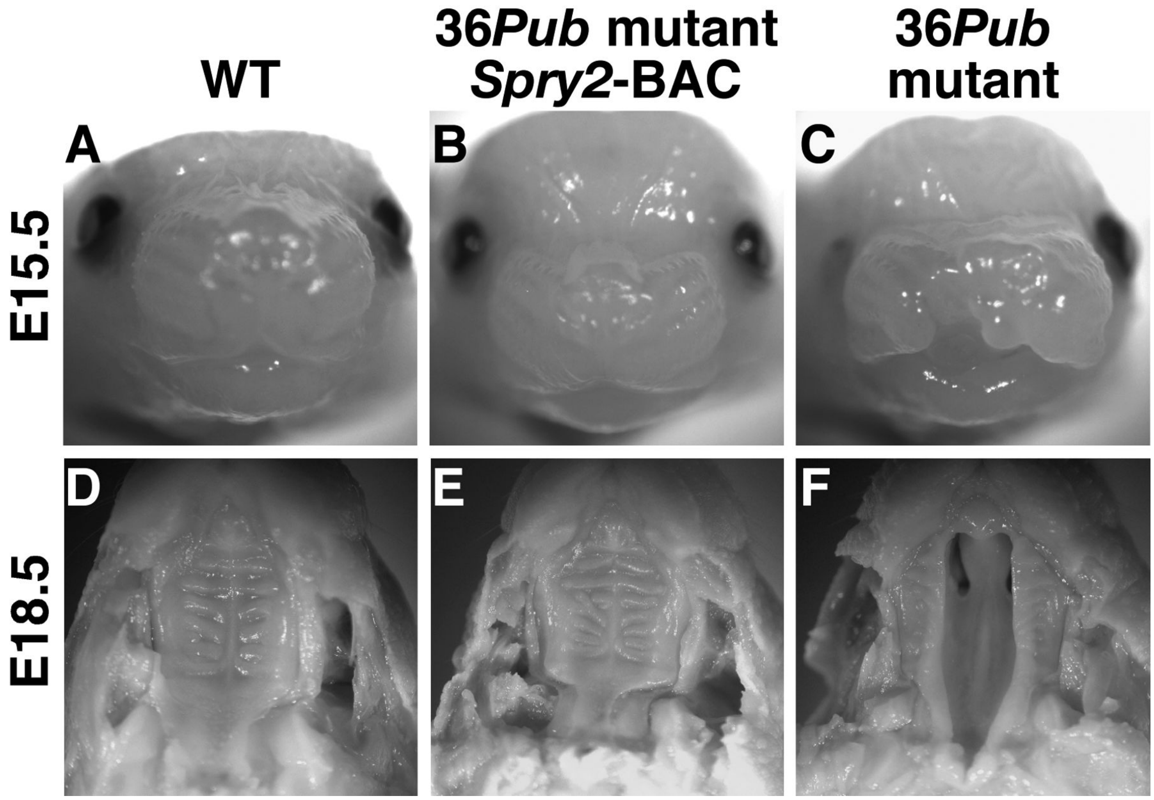

Fig. 4.

Hypomorphic rescue by *Spry2*-BAC transgene of craniofacial defects observed in *36Pub* mutant mice. (A-C) *Spry2*-BAC transgene rescues defects of the primary palate. E15.5 wildtype (A) and E15.5 *Spry2*-BAC hemizygous, *36Pub* mutant mice (B) show normal development of the primary palate and lip whereas E15.5 *36Pub* mutant mice (C) exhibit facial clefting. (D-F) Rescue of cleft palate at E18.5 is shown by complete closure in wildtype (D) and *Spry2*-BAC hemizygous, *36Pub* mutant mice (E) compared with cleft palate in the *36Pub* mutant (F).

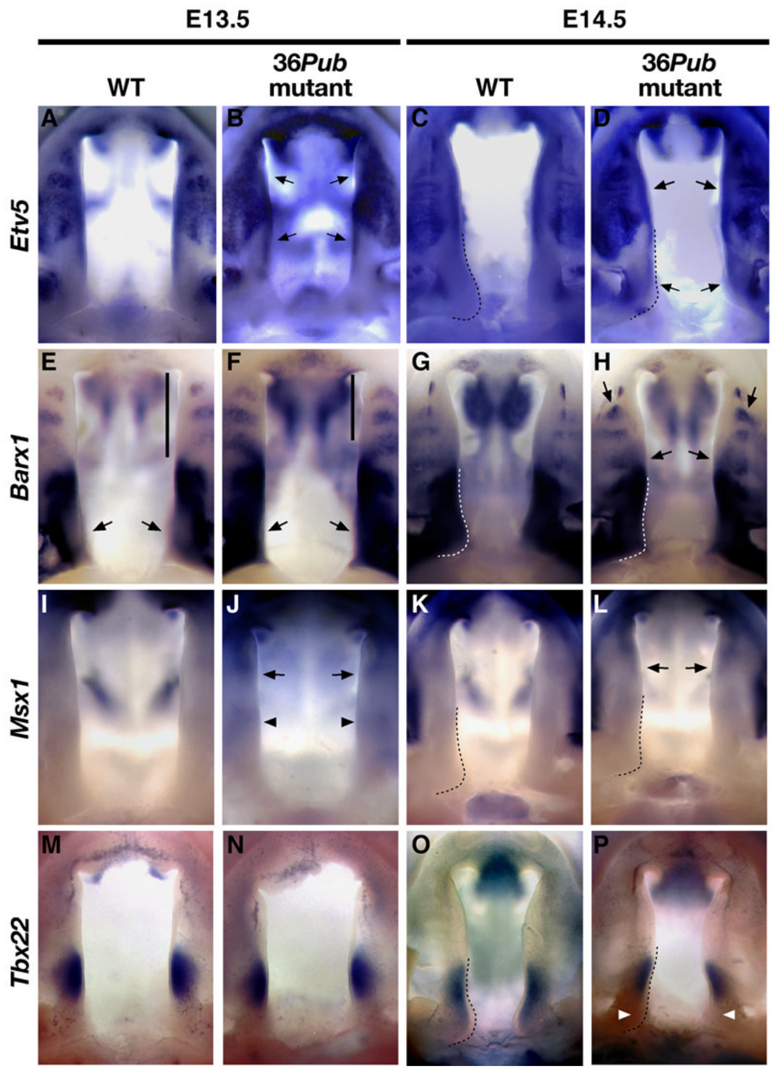

Fig. 5.

Altered gene expression along the anterior-posterior axis of the *36Pub* mutant palate. (A-D) *Etv5* expression. (A) *Etv5* expression in the E13.5 wildtype palate is restricted to segmented domains in the anterior two-thirds of the epithelium and in the mesenchyme to the medial aspect of the vertical shelf. Expression of *Etv5* in E13.5 *36Pub* (B) mutant is upregulated and expanded in both the epithelial and mesenchymal domains (arrows). (C) Wildtype expression of *Etv5* in the mesenchyme at E14.5 becomes restricted to the anterior two-thirds of the palatal shelf. In E14.5 *36Pub* mutants (D) *Etv5* remains upregulated and expanded in the epithelium and ectopic mesenchymal expression extends into the posterior of the shelves (arrows in D). (E-H) *Barx1* expression. (E) E13.5 wildtype *Barx1* expression is restricted to segmented domains in the anterior epithelium and to the mid-posterior half of the palatal mesenchyme. In the E13.5 *36Pub* mutant (F) *Barx1* expression is elevated in the anterior epithelium and the posterior mesenchymal domain is expanded. Note arrows marking elevated medial domain of *Barx1* in the posterior of mutants compared to wildtype, also compare bars marking length of *Barx1* negative domains in the anterior mesenchyme. (G) *Barx1* in the E14.5 wildtype is expressed in anterior epithelium and posterior mesenchyme and elevated and expanded expression domains persist in the E14.5 *36Pub* mutant (arrows in H). (I-L) *Msx1* expression. (I) *Msx1* is expressed at low levels in the mesenchyme in the anterior third of the E13.5 wildtype palate.

NIH-PA Author Manuscript

NIH-PA Author Manuscript

(J) The *36Pub* mutant palate shows elevated *Msx1* expression anteriorly (arrows) and ectopic expression in the mid-posterior palate (arrowheads). (K) Weak *Msx1* expression in the E14.5 wildtype anterior palate compared with (L) continued elevated expression in the E14.5 *36Pub* mutant palate (arrows). (M-P) *Tbx22* expression. (M) *Tbx22* is strongly expressed in the mesenchyme of the mid-posterior of the E13.5 wildtype palate. (N) We detected no difference in *Tbx22* expression in the E13.5 *36Pub* mutant. (O) At E14.5 as the posterior palate initiates medially directed growth the wildtype *Tbx22* expression domain extends to the posterior end of the palate. (P) Failure to initiate posterior expansion of *Tbx22* expression at E14.5 (white arrowheads) is associated with altered morphological progression of the posterior palate in *36Pub* mutants. Dashed lines outline posterior palatal shelf to highlight altered morphology of E14.5 *36Pub* mutants.

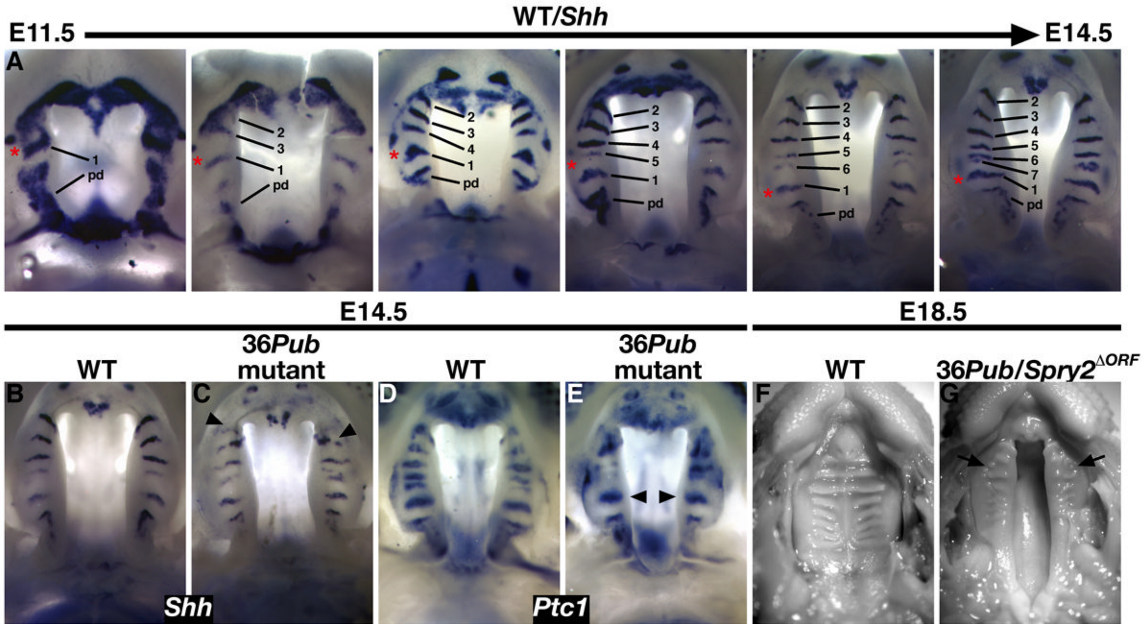

Fig. 6.

Shh expression in the rugae highlights regional growth of the palate and *Shh* expression is altered by loss of *Spry2*. (A) *Shh* expression on the oral surface of the palatal shelves in wildtype embryos from E11.5 through E14.5. Expression is restricted to stripes corresponding to developing rugae (numbered 1-7) and a posterior domain (pd) corresponding to the presumptive soft palate. The number of *Shh* expressing rugae increases as palate development progresses. Using expression in the molar tooth bud (asterisks) and the first distinct stripe of *Shh* (1) as landmarks illustrates that the relative position of these two domains remains constant whereas the number of rugae increases anterior to this position. Because new rugae are formed just anterior to stripe #1, numbering the rugae in order of their formation places each subsequently formed rugae (#3-7) between the anterior most stripe #2 and the posterior stripe #1. This results in the apparent posterior regression of the rugae forming region and presumptive soft palate relative to the rostral extension of the anterior palate (compare relative A-P positions of red asterisks). (B&C) Well defined domains of *Shh* expression in the rugae of E14.5 wildtype (B), *Shh* expression in the E14.5 *36Pub* mutant palate is both diffuse and fragmented into isolated clumps of expressing cells (arrowheads in C). (D&E) Wildtype expression of *Ptc1* is restricted to the mesenchyme immediately adjacent to the overlying *Shh* domain in the rugae and broadly expressed in a posterior domain (pd) of the mesenchyme of the presumptive soft palate (D). In the E14.5 *36Pub* mutant palate (E) *Ptc1* expression is disorganized and ectopically expressed in expanded domains of the palate. Note that *Ptc1* expression in stripe #1 appears less impacted than in more anterior domains (arrowheads in E). (F&G) Rugae morphology at E18.5. The wildtype palate typically has an orderly array of 7 to 9 rugae, the 3 anterior most of which fuse across the midline (F). Rugae morphology is disorganized and fragmented in the cleft palates of both *36Pub* homozygous (not shown) and 36*Pub*/ *Spry*$^{2\Delta}$ORF compound mutants (arrows in G) at E18.5.

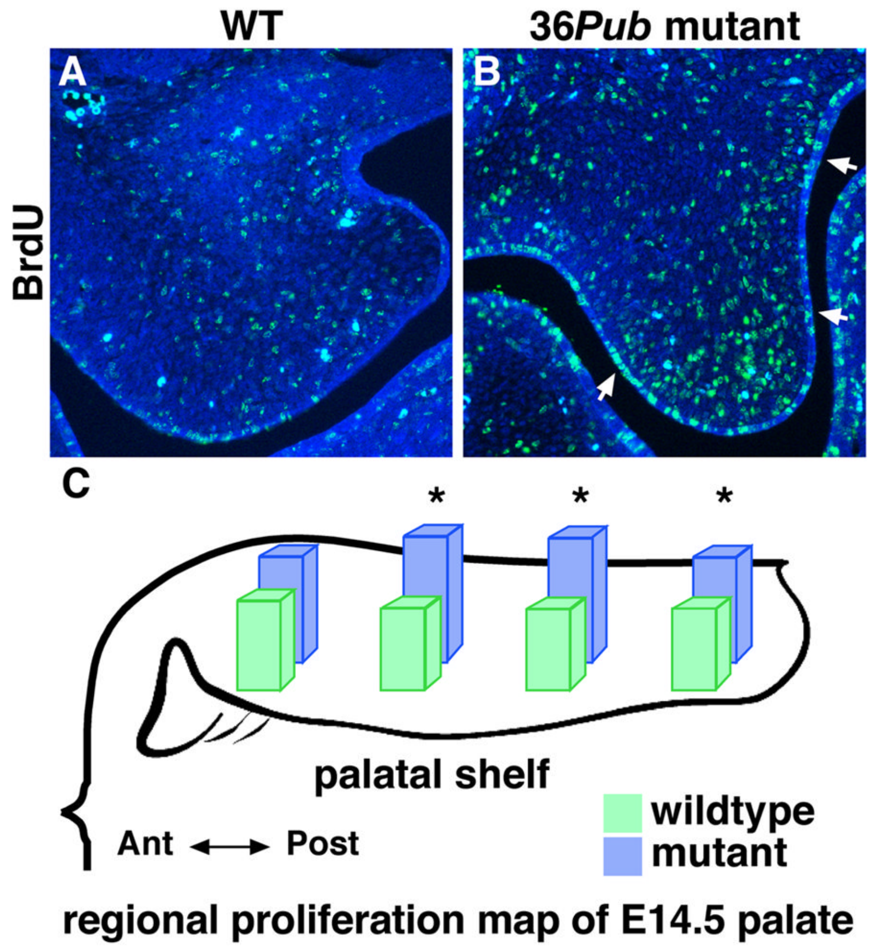

Fig. 7.

Altered proliferation in the *36Pub* mutant palate. Frontal sections in the mid-posterior region of E14.5 wildtype (A) and E14.5 *36Pub* mutant (B) palates show increased proliferation in the mutant shelves. Mitotic cells (green) were detected using a BrdU incorporation assay. Nuclei are counterstained with DAPI (blue). Note increased labeling of mitotic cells throughout both the overlying epithelium and underlying mesenchyme particularly along the medial aspect of the palatal shelf and mesenchyme underlying the MEE (white arrows). (C) A regional proliferation map of the mitotic index along the A-P axis of the palate highlights increased cell proliferation in the mutant palate (asterisks $p<0.05$, see Supplementary Table 1).

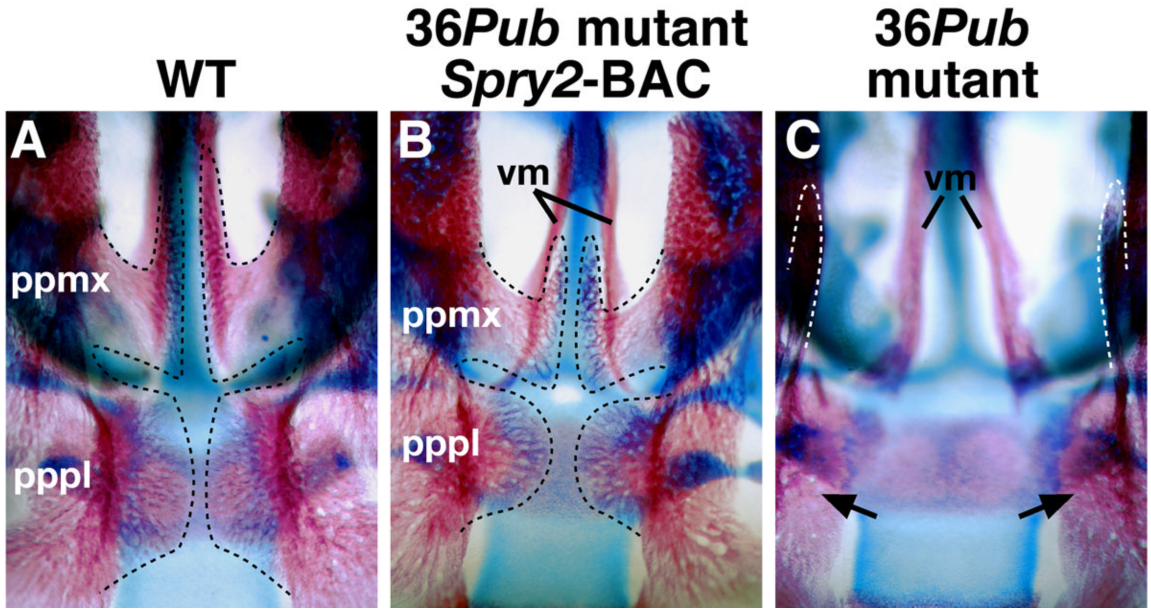

Fig. 8.
Altered morphology of skeletal elements in the *Spry2*-deficient palate. (A-C) E18.5 alcian blue and alizarin red stained skeletal preparations identify a hypomorphic phenotype of reduced skeletal differentiation in *Spry2*-BAC hemizygous, *36Pub* mutant mice. Compared to E18.5 wildtype (A) the palatal processes of the maxilla and palatine bones of the hard palate (outlined in dashed black line in A and B) are reduced in size and show altered morphology in the closed palates of E18.5 *Spry2*-BAC hemizygous, *36Pub* mutant mice (B). In the nontransgenic E18.5 *36Pub* mutant (C) the palatal process of the maxilla is highly hypoplastic (outlined in dashed white line) while the more posterior process of the palatine bone is completely absent (arrows). Abbreviations: ppmx, palatal process of the maxilla; pppl, palatal process of the palatine bone; vm, vomeronasal.

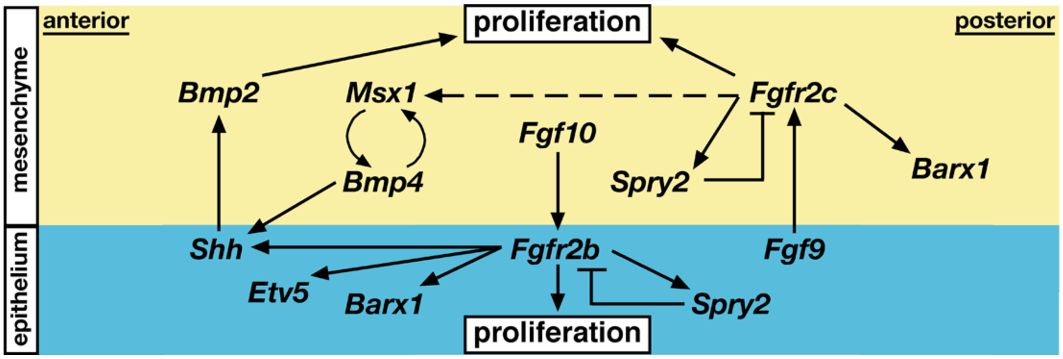

Fig. 9.
Model of epithelial-mesenchymal signaling regulating cell proliferation during palatogenesis. In the anterior palate, mesenchymal proliferation is controlled by a *Bmp4*/*Msx1* feedback loop required for *Shh* and *Bmp2* expression. Proliferation and *Shh* expression in the epithelium is also dependent on *Fgf10* signaling through *Fgfr2b*. *Fgf9* is a candidate for an epithelial source of FGF regulating mesenchymal proliferation and gene expression. The palatal mesenchyme is patterned into anterior *Msx1* and posterior *Barx1* domains. The expression of these genes is responsive to thresholds of FGF signaling. Elevated FGF activity in the absence of *Spry2* antagonism leads to increased proliferation, elevated and expanded *Etv5* and *Barx1* expression, ectopic expression of *Msx1* (dashed arrow), and altered *Shh* expression. Therefore FGF signaling thresholds must be properly modulated to coordinate shelf outgrowth and loss of the FGF antagonist *Spry2* results in perturbations of gene expression, cell proliferation and timing of palatal development.

Table 1

Spry2-BAC rescue and *Spry2*$^{\Delta}$ORF failure to complement facial defects in *36Pub* mutants

Incidence of cleft palate[1]:	*36Pub*/+	*Spry2*$^{\Delta ORF}$/+	36Pub/36Pub	*36Pub/ Spry2*$^{\Delta ORF}$
Spry2-BAC nontransgenic	0/58	0/10	10/12 (83%)	6/17 (35%)
Spry2-BAC line 69 hemizygotes	-	-	1/12 (8%)	-
Spry2-BAC line 2 hemizygotes	-	-	5/12 (42%)	-
Incidence of facial clefting[1]:	*36Pub*/+	*Spry2*$^{\Delta ORF}$/+	36Pub/36Pub	*36Pub/Spry2*$^{\Delta ORF}$
Spry2-BAC nontransgenic	0/58	0/10	19/71 (27%)	0/17
Spry2-BAC line 69 hemizygotes	-	-	0/23	-
Spry2-BAC line 2 hemizygotes	-	-	0/25	-

[1] Cleft palate scored at E18.5; Facial clefting scored in E12.5-E18.5 embryos.